Development of Alzheimer's disease imaging agents for clinical studies

Eun Kyoung Ryu, Xiaoyuan Chen

The Molecular Imaging Program at Stanford (MIPS), Department of Radiology and Bio-X Program, Stanford University School of Medicine, Stanford, California

TABLE OF CONTENTS

1. ABSTRACT

Alzheimer's disease (AD) is a neurodegenerative disease characterized by a progressive loss of neurotransmitters, as well as acetylcholinesterase and nicotinic acetylcholine receptors in the central nervous system that leads to learning and memory deficits, among other problems. The disease is associated with increased production and accumulation extracellular amyloid plaques and neurofibrillary tangles in aging human brain, shown in postmortem exams. New methods for reliable in vivo measurement of brain therefore would be much more ideal. PET and SPECT imaging are sensitive methods for the quantitation of AD biomarkers. The development of molecular imaging agents for AD is critically important in the early diagnosis, neuropathogenesis studies and treatment of AD. A number of potential diagnostic PET and SPECT imaging agents targeting AD have been synthesized and evaluated. Although many agents showed excellent results for in vitro monitoring of the disease, there are only several radioligands with high selectivity and specificity to binding sites and appropriate pharmacokinetics, such as [11C]MP4A, [11C]PMP, [11C]nicotine, 2- or 6-[18F]fluoro-A-85380, [11C]SB-13, [11C]PIB, and [18F]FDDNP, that have been tested in AD patients. Here we review some recent progress and development of AD imaging agents using PET and SPECT in human clinical studies.

2. INTRODUCTION

Alzheimer's disease (AD) was defined by Dr. Alois Alzheimer, a Bavarian psychiatrist, in 1906. It is a progressive neurodegenerative brain disorder of the central nervous system (CNS) and the most common cause of dementia in elderly individuals. The primary risk factor for AD is age. It is characterized by gradual impairments in important cognitive functions, including thinking, memory, learning, and language. Eventually, even the patient's the ability to perform such basic normal daily activities as feeding and dressing oneself will be lost. Although the pathological hallmarks for the disease have long been studied, the precise mechanisms causing the disease remain largely unknown and even controversial. Currently, there are several proposed causes for the disease such as the loss of cholinergic function, and the formation of amyloid plaques and neurofibrillary tangles. In the mid 1970s and 1980s, dementia symptoms associated with malfunctioning neurons synthesizing and releasing acetylcholine (ACh) in the brain emerged as the first clear neurochemical indicia of AD. Researchers noticed that the activity of acetylcholinesterase (AChE) and nicotinic acetylcholine receptors (nAChR) levels are markedly reduced in the cerebral cortex of postmortem brain tissues of AD patients (1, 2). Advances in biochemical pathology later led to the discoveries that with age, amyloid senile plaques and neurofibrillary tangles are abnormally accumulated in the

MP(3- or 4-)A: R = CH$_3$
MP(3- or 4-)P: R = CH$_2$CH$_3$
MP(3- or 4-)IB: R = CH(CH$_3$)$_2$

MP(3- or 4-)OH
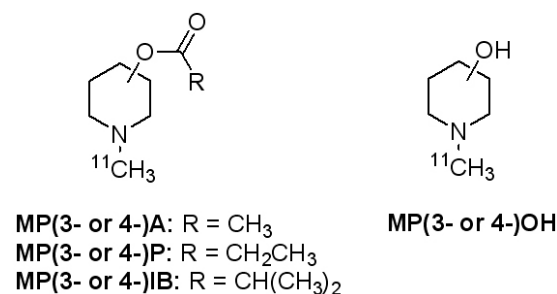
Figure 1. Some representative N-methylpiperidyl ester analogs.

cortical regions, especially in the Alzheimer brain. In vivo imaging of these biomarkers lent support to the hypothesis that effective noninvasive method of determining of these lesions would help make possible not only the early diagnosis of AD, but also the timely monitoring of treatment efficacy. This is particularly important in light of the dramatic increases in the number of people who suffer from AD worldwide, in part due to growing longevity of the population. The obvious limitations of postmortem brain studies have already prompted several attempts to develop agents for in vivo imaging. More recently, sensitive diagnostic tools to recognize early stages of the disease have been developed (3). Positron emission tomography (PET) and single-photon emission computed tomography (SPECT), for instance, are powerful methods that hold the promise to help researchers understand the structural and behavioral foundations of AD. Although many methods to detect AD by staining postmortem brain tissue exist, PET and SPECT are better modalities with the required selectivity and sensitivity (pico- to nanomolar range) to measure the density and interactions of specific binding sites in vivo. These techniques can also be used in kinetic studies that monitor the distribution of radionuclides and map biochemical and physiological processes in the brain. The next advances in diagnosing and treating AD will therefore depend significantly on the use of novel neuronuclear imaging techniques under development and evaluation, some of which are described in this paper.

For a PET or SPECT probe to be successfully employed for brain imaging in the AD patients, several criteria must be met. First, the probe must have high specificity and selectivity for the relevant binding sites and low rates of binding to brain tissue not containing the receptor of interest. Second, the candidate radioligand should be capable of rapidly crossing the blood-brain barrier (BBB) in adequate concentrations to permit access for tracers, as well as allowing high initial brain uptake and fast clearance of the activity from the brain. Neutral molecules with small size (m.w. < 650) and reasonable lipophilicity (log P = 0.1 – 3.5) tend to cross BBB readily. Third, the probe should be able to distinguish AD brain tissue from brain tissue of an age-matched, cognitively normal individual. Lastly, the ligand should be readily labeled with appropriate radionuclides and the labeled probe should be stable in vivo and nontoxic. AChE, nAChR, and Aβ plaque imaging have proven useful in the early diagnosis of AD and the monitoring of its treatment,

including the determination of appropriate clinical doses for newly developed agents (4-7). This review summarizes some of the recent progress and development of AD imaging agents.

3. DETECTION OF CHOLINERGIC SYSTEMS FOR IN VIVO MAPPING OF AD

3.1. Imaging of acetylcholinesterase (AChE)

At the cellular level, there is a marked reduction in the levels of neurotransmitters in the cortex and hippocampus of AD patients due to the loss of neurons (8). The associated decrease in levels of cholinergic neurotransmission has been associated with the cognitive impairment seen in AD patients (9). Particularly important is the depletion of ACh, of which there are two cholinergic marker enzymes, choline acetyltransferase (ChAT) and AChE. ChAT, the enzyme that synthesizes the neurotransmitter ACh, is found in the presynaptic axons. AChE, the enzyme that hydrolyzes ACh, is found in both the cholinergic axons and the cholinoceptive neurons. Significantly, ChAT and AChE activities are greatly reduced in the cortical regions in AD (10-12), and this decreased activity is correlated with the extent of cognitive impairment seen in AD patients (13). Moreover, AChE tends to deposit within the neurofibrillary tangles and amyloid plaques of AD (14). As a result, substantial amount of pharmacological research has involved using AChE inhibitor drugs to attempt to enhance cholinergic neurotransmission level in the synaptic cleft.

There are two different approaches for *in vivo* imaging of AChE. One is to monitor the enzyme activity with radiolabeled AChE substrate; alternatively, one can measure the enzyme density by using radiolabeled AChE inhibitor (15).

Designed to be a radioligand of the metabolic trapping type (16-19), the radiolabeled N-methylpiperidyl esters can also serve as *in vivo* AChE substrates. For example, N-[^{11}C]methylpiperidin-4-yl acetate (MP4A or AMP) and N-[^{11}C]methylpiperidin-4-yl propionate (MP4P or PMP) (Figure 1), are two ACh analogs that are selective, irreversible substrates for AChE and lipophilic ACh ligands. They readily enter the brain by diffusion (K_1) and are selectively hydrolyzed by AChE into the hydrophilic metabolites (k_3), and are then trapped completely in the brain according to the distribution of enzyme activity (Figure 2) (20). [^{11}C]MP4A and [^{11}C]PMP have been studied in AD patients (21, 22). When [^{11}C]MP4A or [^{11}C]PMP was intravenously injected into healthy controls and patients with AD, they showed an average reduction rate of 11-38% in cortical lesions and a reduced estimated AChE activity in comparison with control participants. Moreover, inhibitory effects of donepezil on AChE activity were also seen in the brain of AD patients (Figure 3) (22, 23).

A number of studies have indicated that AChE inhibitors can interfere with the progression of AD. This property has led to the proposed treatments based on the idea that an increase in cholinergic neurotransmission may improve cognition. To evaluate this possibility, many

Table 1. Inhibitory effects of donepezil, physostigmine and tacrine on AChE and BuChE activity

Compound	Activity IC$_{50}$, nM		Ratio of IC$_{50}$ (BuChE/AChE)
	AChE	BuChE	
Donepezil	5.7 ± 0.2	7138 ± 133	1252
Physostigmine	0.68 ± 0.02	8.1 ± 0.3	11.9
Tacrine	80.6 ± 2.5	73.0 ± 0.9	0.9

Adapted with permission from ref. 30.
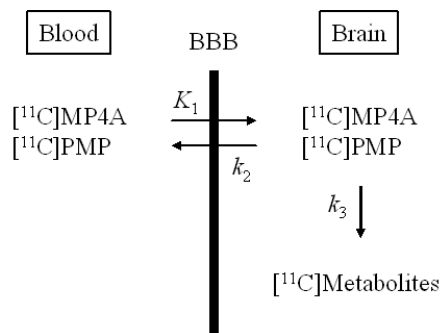
Figure 2. Schematic representation of the three-compartment model of [^{11}C]MP4A and [^{11}C]PMP kinetics in the brain. The entire process is described by three functional parameters: K_1, representing the rate constant of radioligand for transport from blood to brain; k_2, representing the rate constant of radioligand for transport from brain to blood; and k_3, representing the rate constant of radioligand for hydrolysis by AChE.
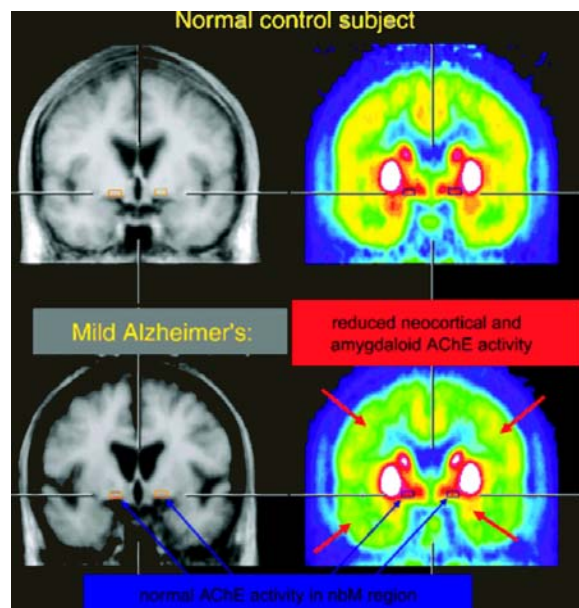
Figure 3. ^{11}C-MP4A PET in mild-to-moderate AD demonstrates reduction in cortex and amygdala but preserved activity in basal forebrain, which suggests a dying-off of cholinergic neurons rather than initial loss of cell bodies. AChE = acetylcholinesterase; nbM = nucleus basalis of Meynert. Adapted with permission from ref. 23.

AChE inhibitor drugs have been radiolabeled with ^{11}C or ^{18}F for PET imaging studies (Figure 4).

Physostigmine, developed by Pfizer, was known to be a potent anti-AChE inhibitor. Physostigmine has higher binding affinity for AChE than AMP or PMP. In primate and rat brains, [^{11}C]physostigmine was found to have a rapid uptake in AChE-rich regions (24). After intravenous injection of [^{11}C]physostigmine (Figure 4) in healthy human volunteers, radioactivity was rapidly taken up in brain tissue and accumulated more in regions rich in AChE, such as the striatum, than in regions poor in AChE, with a target tissue to non-target tissue ratio of about 2 (25). However, it also showed a short biological half-life, which means that the ligand has poor pharmacokinetic parameters for AChE imaging (25). In addition, the radioligand showed lower selectivity of AChE than butyrylcholinesterase (BuChE), and its high lipophilicity led to nonspecific binding in the brain regions (Table 1).

1,2,3,4-Tetrahydro-9-aminoacridine (tacrine, THA/Cognex) was the first drug approved by the US Food and Drug Administration (FDA) for the treatment of AD. Tacrine is a centrally active aminoacridine compound and has been shown to increase brain ACh levels, thereby acting as a reversible AChE inhibitor. Oral administration of tacrine is useful in the long-term palliative treatment of AD patients (26). However, tacrine appears to have lower binding affinity than donepezil and physostigmine for AChE (Table 1). In order to study the localization and pharmacology of AChE binding sites in the brain, tacrine was labeled with C-11 for PET imaging (Figure 4). Even though tacrine is known to be a potent therapeutic agent for patients suffering from AD, the regional distribution of the [11C]methyl-tacrine showed low selectivity in the brain of rats and baboons (14). Tacrine was also reported to have side effects on the peripheral nervous system and hepatotoxicity (27, 28), which may further limit its use.

Donepezil hydrochloride, the second drug approved by the FDA, was developed and is currently used worldwide for the treatment of AD. This agent has emerged as a new class of reversible AChE inhibitor with an N-benzylpiperidine and an indanone moiety that exhibits a high affinity and selectivity for AChE (IC$_{50}$ = 5.7 nM) (Table 1) (29-32). However, ^{18}F-labeled donepezil and 5- or 6-[^{11}C-methoxy]donepezil did not have significantly different regional distributions of AChE in the animal brains (33-35), probably because these ligands have no specific binding to the AChE or specific binding sites in vivo in the brain.

Recent studies have also shown that N-benzylpiperidine lactam benzisoxazoles are potent, selective AChE inhibitors (IC$_{50}$ = 0.33-3.6 nM) and are selective for AChE over BuChE (> 1,000-fold) (36). In particular, AChE activities of 5,7-dihydro-3-[2-[1-(phenylmethyl)-4-piperidinyl]ethyl]-6H-pyrrolo[3,2-f]-1,2-benzisoxazol-6-one) (CP-118,954) and 5,7-dihydro-7-methyl-3-[2-[1-(phenylmethyl)-4-piperidinyl]ethyl]-6H-pyrrolo[3,2-f]-1,2-benzisoxazol-6-
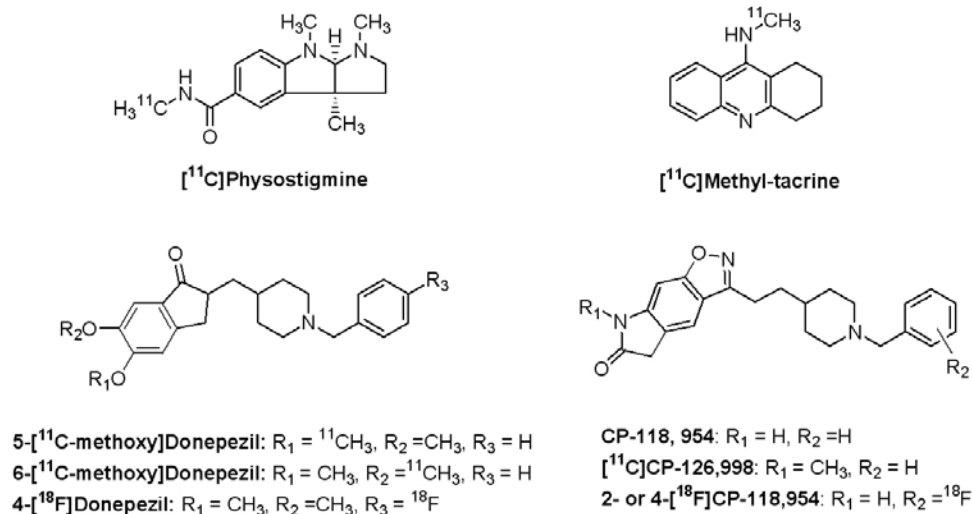
Figure 4. Some representative radiolabeled AChE inhibitors.

one (CP-126,998) displayed high anti-AChE activity (IC_{50} = 0.33 and 0.48 nM, respectively), and low binding affinity for BuChE (IC_{50} = 7200 and 4500 nM, respectively). [^{11}C]CP-126,998 was obtained by the N-alkylation ^{11}C-labeling of lactam nitrogen of CP-118,954 with good radiochemical yield and high specific radioactivity (Figure 4). In vivo mouse biodistribution studies revealed that [^{11}C]CP-126,998 was localized most prominently in the striatum (6.1 % ID/g at 5 min), a region known to be rich in AChE, and declined by approximately 50% at 120 min (3.14 % ID/g). Competitive blocking studies using a variety of AChE inhibitors (diisopropylfluorophosphate, tacrine, and CP-118,954) significantly inhibited the uptake in a dose-dependent manner, verifying the specificity of the PET radiotracer for brain AChE (35, 37). When [^{11}C]CP-126,998 was investigated in healthy human subjects, PET study showed that the radioligand readily crosses the BBB and there is a good correlation between the radioligand and AChE brain concentration of the postmortem data from AD patients (38, 39). However, in the blocking studies with donepezil, the radioactivity was reduced in all brain regions, which suggests that the radioligand provided nonspecific binding in the brain (40).

Taken together, the numerous studies described above amply demonstrate that the changes in cholinergic neurotransmission such as AChE binding sites due to the progression of AD can be monitored using radiolabeled AChE substrates or inhibitors.

3.2. Examination of nicotinic acetylcholine receptors (nAChRs) for AD

Receptors, usually proteins, have a prominent role in brain function, as they are the binding sites for neurotransmission, where presynaptically released neurotransmitters interact with their postsynaptic receptors, which is the basis for all cognitive and sensory processes. Also, the receptors located on the presynaptic membrane are important for negative feedback and for reuptake of transmitters and on cell bodies. Receptors can be characterized by their affinity and density in specific brain areas and affected by many pathologic conditions. Imaging of the regional distribution of receptors may provide a relevant insight into the organization of functional networks in the brain. nAChRs, which mediate excitatory neurotransmission in brain, are known to participate in various neurophysiological functions (41). For example, nAChR subtypes provide information useful in designing selective nAChR ligands targeting a variety of CNS disorders (2) and are involved in tobacco dependence (42, 43). The nAChRs are known to have nine α and three β subunits in the central and peripheral nervous systems (44). The high affinity nicotinic receptors were identified as α4β2 (45). The α4β2 nAChR plays an important physiological role in the brain, including neurodegenerative disorders (46). The severe loss of nAChRs, for instance, is a histopathological hallmarks of AD noted in patients (47). Early in the course of AD, a reduced uptake of radioligands to nicotinic receptors in frontal and temporal cortex has been observed relative to age-matched healthy control subjects (48). Therefore, noninvasive and quantitative imaging of nAChRs would provide a better understanding on the pathology of AD. A number of radioligands have been developed as PET agents for imaging nAChRs (Figure 5). So far, only 11C-nicotine has been tested in AD patients. 2-[18F]fluoro-A-85380 and 6-[18F]fluoro-A-85380 have been tested in healthy subjects.

Nicotine, an agonist of nicotinic receptors, was the first labeled with ^{11}C for PET imaging of nAChRs for early diagnosis of AD (49, 50). In vitro autoradiography studies with [^{3}H]nicotine showed that nAChRs were significantly reduced in caudate and putamen in AD compared to age-matched controls (51). PET imaging further demonstrated significantly lower binding of [^{11}C]nicotine in the frontal cortex, temporal cortex and

[11C]Nicotine   **(-)-Epibatidine**

[18F]FPH   **6-[18F]fluoro-A-85380**
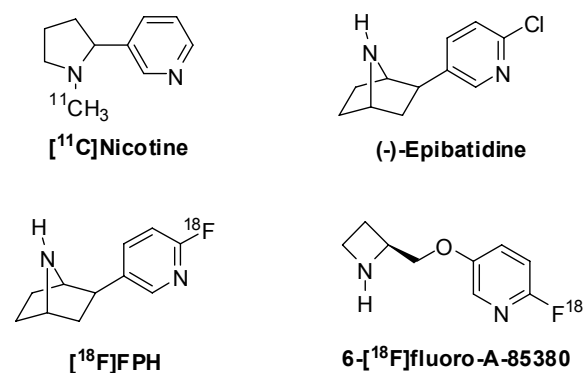
Figure 5. Some representative radiolabeled nAChR ligands.
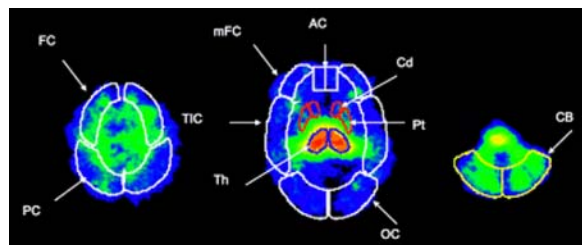
Figure 6. Two-dimensional standardized regions of interest are placed on 3 representative transverse images of 5-[123I]iodo-A-85380 using SPECT. FC = frontal cortex; PC = parietal cortex; mFC = medial frontal cortex; TIC = temporoinsular cortex; AC = anterior cingulate; OC = occipital cortex; Cd = caudate; Th = thalamus; Pt = putamen; CB = cerebellum. Adapted with permission from ref. 69.

hippocampus of AD patients compared with controls (48). high level of nonspecific binding, rapid metabolism and clearance (50, 52, 53). A search for more specific nAChR radioligand is thus needed.

Epibatidine ((+)-exo-2-(2-chloro-5-pyridyl)-7-azabicyclo[2.2.1]heptane), an alkaloid extracted from the skin of the Ecuadorian poisonous frog *Epipedobates tricolor*, was found to inhibit the binding of [3H]nicotine and [3H]cytisine (54-57). A highly potent 18F-labeled analog of epibatidine, (+/-)-exo-2-(2-[18F]fluoro-5-pyridyl)-7-azabicyclo[2.2.1]heptane ([18F]FPH) has subnanomolar affinity for nAChR. The distribution of [18F]FPH in the mouse brain matched with nAChR densities determined in postmortem autoradiographic studies and showed slow clearance from the brain (58, 59). Pretreatment of nAChR inhibitors significantly inhibited [18F]FPH binding in the thalamus and superior colliculus but not in cerebellum, whereas drugs that interact with binding sites other than ACh recognition sites of nAChR had no effect on [18F]FPH accumulation in any of the brain regions examined (58). Although the radioligand showed high brain uptake and high specificity, the radioligand would not be worthwhile for PET studies in human because of the high toxicity (60).

The derivatives of 3-[2(S)-2-azetidinylmethoxy]pyridine (A-85380) have also been

reported to have subnanomolar affinity for nAChRs (Table 2) and lower toxicity than epibatidine (61-64). Several radiohalogenated A-85380 derivatives have been identified as potent probes for studying nAChRs (65-69). The [18F]fluoro, [76Br]bromo, and [123I]iodo derivatives have been examined to have high binding and high specificity for the nAChRs-rich thalamus in monkey and healthy nonsmoker subjects (Figure 6) (61, 68, 69). Especially, 2- or 6-[18F]fluoro-A-85380 displayed reasonable kinetics and higher specific binding for PET studies in baboon (ratio of thalamus to cerebellum = 2.5 - 3.5 at 180 min) (70). In human subjects for imaging nAChR, these include the high affinity and selectivity for the α4β2 nicotinic receptors, fast binding kinetics, and high specific binding (68, 71, 72).

4. *IN VIVO* IMAGING OF AMYLOID PLAQUES FOR EARLY DIAGNOSIS OF AD

Although the cause of AD is still unclear, it is well established that abnormal overproduction and deposition of extracellular β-amyloid plaques (73-75) and neurofibrillary tangles within nerve cell bodies are pathological hallmarks of AD. Glenner *et al.* (73) originally identified amyloid deposits from Alzheimer brain and the Aβ peptide was recognized as the subunit of the plaque amyloid. The Aβ plaques are composed of a 39-43 amino acid-long β-amyloid peptide (76-79) generated from a larger β-amyloid precursor protein (80). Neurofibrillary tangles are aggregates of the abnormal hyperphosphorylated tau protein (81). The highly hydrophobic peptides are spontaneously aggregated and are neurotoxic (82-84). The development of β-amyloid plaques in the brain may cause physical damage to axons, and the abnormally prolonged stimulation of the neuronal response to this kind of injury ultimately results in the profound cytoskeletal alterations that underlie neurofibrillary pathology and neurodegeneration. Therapeutically, inhibition of the neuronal reaction to physical trauma may be a useful neuroprotective strategy in the early stages of AD (85). Therefore, *in vivo* imaging of amyloid plaques may be useful for diagnosis and evaluation of progression of AD patients. A number of research groups have worked to develop radiolabeled β-amyloid plaque imaging agents (Figure 7). Although most of the ligands showed excellent *in vitro* properties for Aβ aggregates, they were limited by penetration of BBB, poor brain uptake, high non-specific binding and low specific binding. Among these, [11C]SB-13, [11C]PIB and [18F]FDDNP have been applied to AD patients using PET (86-88).

It is known that fluorescent dyes can be used to stain senile plaques and neurofibrillary tangles in postmortem AD brain sections (89, 90). For instance, Chrysamine G (CG) and Congo red (CR), which have highly conjugated symmetric structures, can cross the BBB in normal mice and display low toxicity (91). The K_i values to Aβ aggregates of CG and CR are 370 and 2800 nM, respectively (92). 99mTc-labeled CG and CR derivatives (93) were found to bind Aβ amyloid fibrils produced *in vitro* and capable of labeling amyloid plaques in AD brain sections.(94) However, these radioligands did not cross BBB and had very poor brain uptake.

Table 2. The binding (+)-epibatidine and A-85380 derivatives of for nAChR [from ref. 61 with permission].

Compound	K_i^1 (pM)
(+)-Epibatidine	8.4 ± 0.2
A-85380 (R = H)	17 ± 1
R = 2-F	46 ± 5^2
R = 2-Cl	$(8.4 ± 0.6) \times 10^{3}$ [3]
R = 2-Br	$(240 ± 10) \times 10^3$
R = 2-I	$>1 \times 10^6$
R = 5-F	25 ± 1
R = 5-Cl	30 ± 3
R = 5-Br	21 ± 1
R = 5-I	11 ± 1
R = 6-F	25 ± 3
R = 6-I	150 ± 8

[1] Values represent mean ± SEM obtained from n independent experiments where n = 6-9, except for compound of R = 2-I where n = 3. [2] K_i = 150 pM against [^{3}H]cytosine. [3] K_i = 2.5 nM against [^{3}H]cytosine.

Recently, the radioiodinated styrylbenzene derivatives were shown to selectively bind to Aβ aggregates and readily cross the intact BBB. (E,E)-1-Iodo-2,5-bis(3-hydroxycarbonyl-4-hydroxy)styrylbenzene (ISB), and (E,E)-1-iodo-2,5-bis(3-hydroxycarbonyl-4-methoxy)styrylbenzene, (IMSB) were designed by replacing the diazo group of CG with a simple vinyl group and substituting phenyl for the diphenyl group, which decreases the molecular size and increases the brain uptake. In vitro binding studies of these ligands showed excellent binding affinities with K_d values of 0.08 and 0.13 nM for aggregates of Aβ(1-40) and 0.15 and 0.73 nM for aggregates of Aβ(1-42), respectively. However, biodistribution studies in normal mice after intravenous injection showed that these radioligands do not cross BBB, either (95).

The 4-N-methylamino-4'-hydroxystilbene (SB-13) is also derived from CR and has been used to examine Aβ plaques in postmortem AD brain sections (86). In vitro binding studies using [^{3}H]SB-13 as radioligand showed a K_d value of 2.4 nM for AD cortical homogenates. Autoradiography also showed specific binding of the radioligand in the cortical gray matter, which is correlated with the distribution of amyloid plaques in these brain specimens, as confirmed by thioflavin-S staining. Contrary to expectation, low specific binding in cortical tissue homogenates of age-matched control brain was found (96). SB-13 can be readily labeled with ^{11}C and ^{18}F for PET imaging studies (97, 98). Initial human studies showed that [^{11}C]SB-13 accumulates more in the frontal cortex of AD patients as compare to age-matched healthy controls. The relative cortical uptake pattern of [^{11}C]SB-13 is similar to [^{11}C]PIB (86).

Highly conjugated thioflavin-T, based on benzothiazole and relatively small in molecular size, is also commonly used as a dye for staining the Aβ aggregates in the AD brain. However, the thioflavins contain an ionic quaternary amine that prohibits the penetration of BBB. Therefore, neutral derivatives of thioflavin-T have been developed for *in vivo* imaging of Aβ plaques (99, 100).

Benzothiazole aniline (BTA) analogues are series of neutral derivatives of thioflavin-T with reported high affinity for aggregated amyloid and reasonable lipophilicities for crossing the BBB (99, 101). In particular, [N-methyl-^{11}C]-2-(4'-methylaminophenyl)-6-hydroxylbenzothiazole ([^{11}C]6-OH-BTA-1) has been studied extensively in both preclinical and clinical settings (99-103). Scientists at the University of Pittsburgh and the Uppsala University co-developed this compound. It was given the Uppsala University PET center code of "Pittsburgh Compound-B' or simply, PIB (Figure 8).

[^{11}C]PIB had high binding affinity for homogenates of postmortem AD frontal cortex and synthetic Aβ(1-40) fibrils (K_d = 1.4 nM and 4.7 nM, respectively). The radioligand had high initial uptake in normal mouse brain and rapid clearance from the non-binding sites. It also indicated specific binding of amyloid plaques in transgenic mouse model of AD and cleared rapidly from the normal brain tissue (99). PET imaging studies of baboons also showed similar pattern (100). The radioligand was then used to image amyloid plaques in patients and showed significantly greater cortical uptake of amyloid deposits in AD patients than in control healthy volunteers. High accumulations in parietal, temporal and occipital cortices and striatum were also observed (Figure 9) (88). Amyloid deposits in these regions were confirmed by postmortem studies using silver stains, antibodies to Aβ, or thioflavin-S (104, 105). Polar metabolites appeared rapidly in the plasma, but the metabolites are unlikely to enter the human brain, which is consistent with findings in the rodents (100).

A few other neutral and lipophilic thioflavin derivatives, such as 2-[4'-(dimethylamino)phenyl]-6-iodobenzothiazole (TZDM) and 2-[4'-(4''-methylpiperazin-1-yl)phenyl]-6-iodobenzothiazole (TZPI), have been labeled with ^{125}I. These radioligands showed good Aβ plaque binding *in vitro* (K_d values of 0.06, and 0.13 nM for aggregates of Aβ(1-40) for [^{125}I]TZDM and [^{125}I]TZPI, respectively). However, these two radioligands showed low brain uptake *in vivo* (0.67 and 1.50 %ID/organ at 2 min post injection, respectively) (95). 2-(4'-Dimethylaminophenyl)-6-[^{125}I]iodobenzoxazole ([^{125}I]IBOX) was synthesized as an improved version of [^{125}I]TZDM. The molecular weight of IBOX is reduced while the lipophilicity is increased by replacement of a sulfur atom of TZDM by an oxygen atom to improve *in vivo* kinetics (log P = 1.85 versus 2.09 for TZDM and IBOX, respectively). *In vitro* binding study showed that they have similar potency for Aβ(1-40) aggregates (K_i = 1.9 nM and 0.8 nM for TZDM and IBOX, respectively). [^{125}I]IBOX displayed slightly higher initial brain uptake in normal mice brain and faster washout from the brain as compared to [^{125}I]TZDM (106).

Another thioflavin derivative, 6-iodo-2-(4'-dimethylamino-)phenyl-imidazo[1,2-a]pyridine, IMPY, has been labeled with ^{125}I/^{123}I for SPECT imaging studies. IMPY displayed a good binding affinity for synthetic Aβ
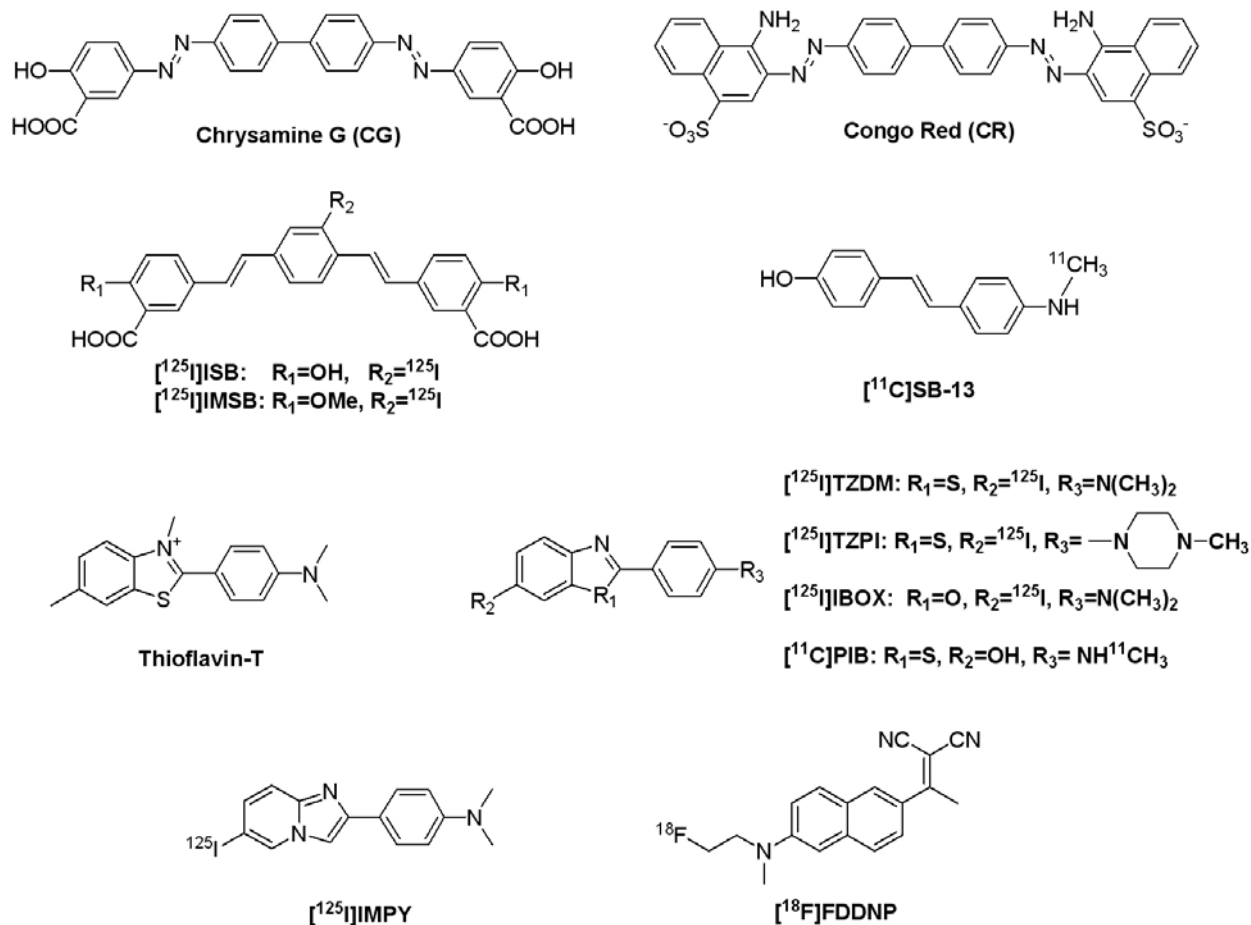
Figure 7. Some representative radiolabeled Aβ plaque specific ligands.

aggregates (K_i = 15 nM) and selective plaque labeling of postmortem AD brain sections (107). [^{125}I]IMPY was also able to label Aβ plaques in transgenic mouse brain sections in the cortical and cerebellar regions and the uptake correlated well with fluorescent staining using Aβ-specific antibody (108).

The neutral and highly lipophilic F-18 radiolabeled fluorescent molecular imaging probes, 2-(1-(6-[(2-fluoroethyl)(methyl)amino]-2-naphthyl)ethylidene)-malononitrile (FDDNP) and 1-(6-[(2-fluoroethyl)(methyl)amino]-naphthalene-2-yl)ethanone (FENE) (log P = 3.92 and 3.13, respectively) had K_d values for the high-affinity binding sites of 0.12 and 0.16 nM, and 1.86 and 71.2 nM for the low-affinity binding sites, respectively. [^{18}F]FDDNP is highly diffusible through the BBB in proportion to blood flow due to its high lipophilicity and localizes to senile plaques and neurofibriallary tangles in the brain of living patients with AD (87, 109, 110). [^{18}F]FDDNP has higher accumulation and slower clearance in the hippocampus of AD patients than normal controls (105, 111). The presence of amyloid plaques and neurofibriallary tangles in this region was also correlated with lower memory performance scores than normal. In a recent study, [^{18}F]FDDNP-PET was also found to be able to differentiate persons with mild cognitive impairment from those with AD and those with no cognitive impairment (112).

5. SUMMARY AND PERSPECTIVE

A large number of radioligands have been developed for AD-specific imaging, most of which showed excellent *in vitro* binding but inferior *in vivo* binding due to the poor penetration of these compounds through intact BBB. Only a few of the compounds have shown promise and been tested in healthy volunteers and AD patients.

To map brain AChE, the lipophilic N-methylpiperidyl ester substrates [^{11}C]AMP and [^{11}C]PMP were shown to readily cross the BBB and hydrolyze in the brain. The metabolites were thus trapped and distributed in the brain according to the distribution of enzyme activity. Radiolabeled AChE inhibitors such as N-benzylpiperidine lactam benzisoxazole derivatives have excellent anti-AChE activity at sub-nanomolar range and radioactivity distribution corresponding to the regional distribution of AChE activity measured in postmortem human brains. [^{11}C]Nicotine is a specific α4β2 nAChR agonist with low uptake in the frontal cortex, temporal cortex and hippocampus of AD patients compared with controls. The main problems with [^{11}C]nicotine PET imaging lie in the
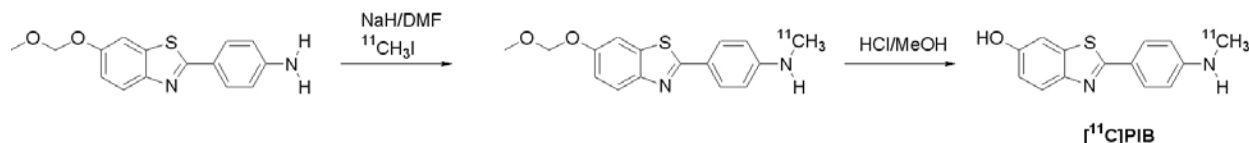
Figure 8. Synthetic scheme of [^{11}C]PIB.
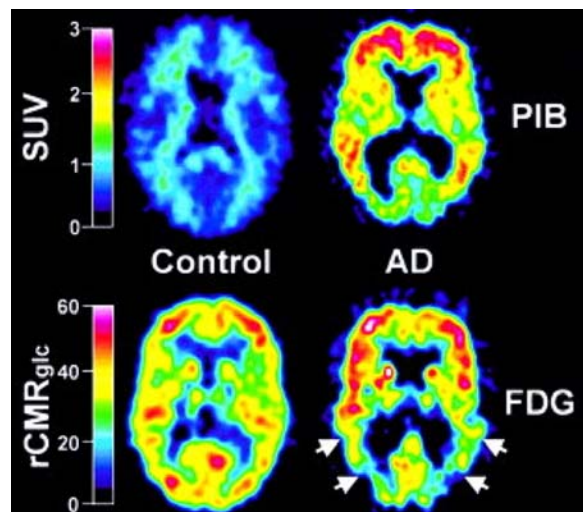
Figure 9. PIB standardized uptake value (SUV) images demonstrate a marked difference between PIB retention in Alzheimer's disease (AD) patients and healthy control (HC) subjects. PET images of a 67-year-old HC subject (left) and a 79-year-old AD patient (MMSE = 21; right). (top) SUV PIB images summed over 40 to 60 minutes; (bottom) ^{18}FDG rCMRglc images (µmol/min/100ml). The left column shows lack of PIB retention in the entire gray matter of the HC subject (top left) and normal ^{18}FDG uptake (bottom left). Nonspecific PIB retention is seen in the white matter (top left). The right column shows high PIB retention in the frontal and temporoparietal cortices of the AD patient (top right) and a typical pattern of ^{18}FDG hypometabolism present in the temporoparietal cortex (arrows; bottom right) along with preserved metabolic rate in the frontal cortex. PIB and ^{18}FDG scans were obtained within 3 days of each other. Adapted with permission from ref. 88.

relatively high level of nonspecific binding, rapid metabolism, and clearance of the tracer. The goal of finding alternative nAChR probes has had only limited success. The Aβ-imaging agents remaining to be developed in clinical studies include [^{11}C]SB-13, [^{11}C]PIB and [^{18}F]FDDNP, all of which can provide *in vivo* brain mapping of human Aβ plaques and are promising for the study of changes in Aβ plaques levels associated with neurodegenerative disease.

AD is difficult to diagnose in its early stages. However, imaging modalities such as PET and SPECT have the potential to help solve this critical problem and thus stimulate the development of novel drugs targeting AD. A number of AD-related biomarkers are being

developed and evaluated. The AChE, nAChR and Aβ plaques described in

this review seem to be close to ideal biomarkers, if they can be safely and successfully applied in additional human trials. There are other biomarkers relevant to the diagnosis of AD. For example, apolipoprotein E (ApoE) is well known as a genetic risk factor for AD (113-115). Several studies also indicate that the overexpression of cyclooxygenase can lead to AD (116, 117). These may be potential targets for noninvasive imaging of AD at early stages. Identifying the molecular events and signaling pathways unique for the very early stages of AD development and progression (before the amyloid plaques have deposited) is crucial for AD to be successfully treated. The continuing development of techniques capable of capturing the molecular events earlier than those currently feasible, as described in this paper, is a highly promising avenue to overcome the challenges that remain ahead in the fight against AD.

6. ACKNOWLEDGMENT

7. REFERENCES

1. K.A. Frey, S. Minoshima, D.E. Kuhl: Neurochemical imaging of Alzheimer's disease and other degenerative dementias. *Q J Nucl Med* 42, 166-78 (1998)

2. E.D. London, S.B. Waller, J.K. Wamsley: Autoradiographic localization of [3H]nicotine binding sites in the rat brain. *Neurosci Lett* 53, 179-84 (1985)

3. Z. Walker, R.W. Walker: Imaging in neurodegenerative disorders: recent studies. *Curr Opin Psychiatry* 18, 640-6 (2005)

4. L. Cai, R.B. Innis, V.W. Pike: Radioligand development for PET imaging of β-amyloid (A β)--current status. *Curr Med Chem* 14, 19-52 (2007)

5. A. Lockhart: Imaging Alzheimer's disease pathology: one target, many ligands. *Drug Discov Today* 11, 1093-9 (2006)

6. V. Kepe, S.C. Huang, G.W. Small, N. Satyamurthy, J.R. Barrio: Visualizing pathology deposits in the living brain of patients with Alzheimer's disease. *Methods Enzymol* 412, 144-60 (2006)

7. A. Nordberg: PET imaging of amyloid in Alzheimer's disease. *Lancet Neurol* 3, 519-27 (2004)

8. L. Parnetti, U. Senin, P. Mecocci: Cognitive enhancement therapy for Alzheimer's disease. The way forward. *Drugs* 53, 752-68 (1997)

9. D.A. Evans, H.H. Funkenstein, M.S. Albert, P.A. Scherr, N.R. Cook, M.J. Chown, L.E. Hebert, C.H. Hennekens, J.O. Taylor: Prevalence of Alzheimer's disease in a

community population of older persons. Higher than previously reported. *JAMA* 262, 2551-6 (1989)

10. P. Davies, A.J. Maloney: Selective loss of central cholinergic neurons in Alzheimer's disease. *Lancet* 2, 1403 (1976)

11. J.T. Coyle, D.L. Price, M.R. DeLong: Alzheimer's disease: a disorder of cortical cholinergic innervation. *Science* 219, 1184-90 (1983)

12. O.J. Vogels, C.A. Broere, H.J. ter Laak, H.J. ten Donkelaar, R. Nieuwenhuys, B.P. Schulte: Cell loss and shrinkage in the nucleus basalis Meynert complex in Alzheimer's disease. *Neurobiol Aging* 11, 3-13 (1990)

13. E.K. Perry, B.E. Tomlinson, G. Blessed, K. Bergmann, P.H. Gibson, R.H. Perry: Correlation of cholinergic abnormalities with senile plaques and mental test scores in senile dementia. *Br Med J* 2, 1457-9 (1978)

14. B. Tavitian, S. Pappata, S. Bonnot-Lours, C. Prenant, A. Jobert, C. Crouzel, L. Di Giamberardino: Positron emission tomography study of $[^{11}C]$methyl-tetrahydroaminoacridine (methyl-tacrine) in baboon brain. *Eur J Pharmacol* 236, 229-38 (1993)

15. H. Shinotoh, K. Fukushi, S. Nagatsuka, T. Irie: Acetylcholinesterase imaging: its use in therapy evaluation and drug design. *Curr Pharm Des* 10, 1505-17 (2004)

16. T. Irie, K. Fukushi, H. Namba, M. Iyo, H. Tamagami, S. Nagatsuka, N. Ikota: Brain acetylcholinesterase activity: validation of a PET tracer in a rat model of Alzheimer's disease. *J Nucl Med* 37, 649-55 (1996)

17. T. Irie, K. Fukushi, Y. Akimoto, H. Tamagami, T. Nozaki: Design and evaluation of radioactive acetylcholine analogs for mapping brain acetylcholinesterase (AchE) in vivo. *Nucl Med Biol* 21, 801-8 (1994)

18. M.R. Kilbourn, S.E. Snyder, P.S. Sherman, D.E. Kuhl: In vivo studies of acetylcholinesterase activity using a labeled substrate, N-$[^{11}C]$methylpiperdin-4-yl propionate ($[^{11}C]$PMP). *Synapse* 22, 123-31 (1996)

19. H. Namba, T. Irie, K. Fukushi, M. Iyo: In vivo measurement of acetylcholinesterase activity in the brain with a radioactive acetylcholine analog. *Brain Res* 667, 278-82 (1994)

20. T. Shiraishi, T. Kikuchi, K. Fukushi, H. Shinotoh, S. Nagatsuka, N. Tanaka, T. Ota, K. Sato, S. Hirano, S. Tanada, M. Iyo, T. Irie: Estimation of plasma IC_{50} of donepezil hydrochloride for brain acetylcholinesterase inhibition in monkey using N-$[^{11}C]$methylpiperidin-4-yl acetate ($[^{11}C]$MP4A) and PET. *Neuropsychopharmacology* 30, 2154-61 (2005)

21. N. Tanaka, K. Fukushi, H. Shinotoh, S. Nagatsuka, H. Namba, M. Iyo, A. Aotsuka, T. Ota, S. Tanada, T. Irie: Positron emission tomographic measurement of brain acetylcholinesterase activity using N-$[^{11}C]$methylpiperidin-4-yl acetate without arterial blood sampling: methodology of shape analysis and its diagnostic power for Alzheimer's disease. *J Cereb Blood Flow Metab* 21, 295-306 (2001)

22. M. Iyo, H. Namba, K. Fukushi, H. Shinotoh, S. Nagatsuka, T. Suhara, Y. Sudo, K. Suzuki, T. Irie: Measurement of acetylcholinesterase by positron emission tomography in the brains of healthy controls and patients with Alzheimer's disease. *Lancet* 349, 1805-9 (1997)

23. W.D. Heiss, K. Herholz: Brain receptor imaging. *J Nucl Med* 47, 302-12 (2006)

24. B. Tavitian, S. Pappata, A.M. Planas, A. Jobert, S. Bonnot-Lours, C. Crouzel, L. DiGiamberardino: In vivo visualization of acetylcholinesterase with positron emission tomography. *Neuroreport* 4, 535-8 (1993)

25. S. Pappata, B. Tavitian, L. Traykov, A. Jobert, A. Dalger, J.F. Mangin, C. Crouzel, L. DiGiamberardino: In vivo imaging of human cerebral acetylcholinesterase. *J Neurochem* 67, 876-9 (1996)

26. W.K. Summers, L.V. Majovski, G.M. Marsh, K. Tachiki, A. Kling: Oral tetrahydroaminoacridine in long-term treatment of senile dementia, Alzheimer type. *N Engl J Med* 315, 1241-5 (1986)

27. W.K. Summers, A.L. Koehler, G.M. Marsh, K. Tachiki, A. Kling: Long-term hepatotoxicity of tacrine. *Lancet* 1, 729 (1989)

28. B. Beermann: Side effects of long acting cholinesterase inhibitors. *Acta Neurol Scand Suppl* 149, 53-4 (1993)

29. H. Sugimoto, Y. Yamanishi, Y. Iimura, Y. Kawakami: Donepezil hydrochloride (E2020) and other acetylcholinesterase inhibitors. *Curr Med Chem* 7, 303-39 (2000)

30. H. Sugimoto, Y. Iimura, Y. Yamanishi, K. Yamatsu: Synthesis and structure-activity relationships of acetylcholinesterase inhibitors: 1-benzyl-4-[(5,6-dimethoxy-1-oxoindan-2-yl)methyl]piperidine hydrochloride and related compounds. *J Med Chem* 38, 4821-9 (1995)

31. H. Sugimoto, H. Ogura, Y. Arai, Y. Limura, Y. Yamanishi: Research and development of donepezil hydrochloride, a new type of acetylcholinesterase inhibitor. *Jpn J Pharmacol* 89, 7-20 (2002)

32. S.L. Rogers, R.S. Doody, R.C. Mohs, L.T. Friedhoff: Donepezil improves cognition and global function in Alzheimer disease: a 15-week, double-blind, placebo-controlled study. Donepezil Study Group. *Arch Intern Med* 158, 1021-31 (1998)

33. F. De Vos, P. Santens, H. Vermeirsch, I. Dewolf, F. Dumont, G. Slegers, R.A. Dierckx, J. De Reuck: Pharmacological evaluation of $[^{11}C]$donepezil as a tracer for visualization of acetylcholinesterase by PET. *Nucl Med Biol* 27, 745-7 (2000)

34. S.Y. Lee, Y.S. Choe, H. Sugimoto, S.E. Kim, S.H. Hwang, K. Lee, Y. Choi, J. Lee, B. Kim: Synthesis and biological evaluation of 1-(4-$[^{18}F]$fluorobenzyl)-4-[(5,6-dimethoxy-1-oxoindan-2-yl)methyl]piperidin e for in vivo studies of acetylcholinesterase. *Nucl Med Biol* 27, 741-4 (2000)

35. Y. Funaki, M. Kato, R. Iwata, E. Sakurai, E. Sakurai, M. Tashiro, T. Ido, K. Yanai: Evaluation of the binding characteristics of [5-^{11}C-methoxy]Donepezil in the rat brain for in vivo visualization of acetylcholinesterase. *J Pharmacol Sci* 91, 105-12 (2003)

36. A. Villalobos, T.W. Butler, D.S. Chapin, Y.L. Chen, S.B. DeMattos, J.L. Ives, S.B. Jones, D.R. Liston, A.A. Nagel, D.M. Nason, et al.: 5,7-dihydro-3-[2-[1-(phenylmethyl)-4-piperidinyl]ethyl]-6H- pyrrolo[3,2-f]-1,2-benzisoxazol-6-one: a potent and centrally-selective inhibitor of acetylcholinesterase with an improved margin of safety. *J Med Chem* 38, 2802-8 (1995)

37. J.L. Musachio, J.E. Flesher, U.A. Scheffel, P. Rauseo, J. Hilton, W.B. Mathews, H.T. Ravert, R.F. Dannals, J.J. Frost: Radiosynthesis and mouse brain distribution studies

of [11C] CP-126,998: a PET ligand for in vivo study of acetylcholinesterase. *Nucl Med Biol* 29, 547-52 (2002)

38. H. Arai, K. Kosaka, O. Muramoto, R. Iizuka: [A biochemical study of cholinergic neurons of the post-mortem brains from the patients with Alzheimer-type dementia]. *Rinsho Shinkeigaku* 24, 1128-35 (1984)

39. J.R. Atack, E.K. Perry, J.R. Bonham, J.M. Candy, R.H. Perry: Molecular forms of acetylcholinesterase and butyrylcholinesterase in the aged human central nervous system. *J Neurochem* 47, 263-77 (1986)

40. B. Bencherif, C.J. Endres, J.L. Musachio, A. Villalobos, J. Hilton, U. Scheffel, R.F. Dannals, S. Williams, J.J. Frost: PET imaging of brain acetylcholinesterase using [11C]CP-126,998, a brain selective enzyme inhibitor. *Synapse* 45, 1-9 (2002)

41. M.W. Decker, J.D. Brioni, A.W. Bannon, S.P. Arneric: Diversity of neuronal nicotinic acetylcholine receptors: lessons from behavior and implications for CNS therapeutics. *Life Sci* 56, 545-70 (1995)

42. A. Pert: Cholinergic and catecholaminergic modulation of nociceptive reactions. Interactions with opiates. *Pain Headache* 9, 1-63 (1987)

43. J.E. Henningfield, P.P. Woodson: Dose-related actions of nicotine on behavior and physiology: review and implications for replacement therapy for nicotine dependence. *J Subst Abuse* 1, 301-17 (1989)

44. V. Itier, D. Bertrand: Neuronal nicotinic receptors: from protein structure to function. *FEBS Lett* 504, 118-25 (2001)

45. C.M. Flores, S.W. Rogers, L.A. Pabreza, B.B. Wolfe, K.J. Kellar: A subtype of nicotinic cholinergic receptor in rat brain is composed of α4 and β2 subunits and is up-regulated by chronic nicotine treatment. *Mol Pharmacol* 41, 31-7 (1992)

46. F. Clementi, D. Fornasari, C. Gotti: Neuronal nicotinic acetylcholine receptors: from structure to therapeutics. *Trends Pharmacol Sci* 21, 35-7 (2000)

47. P.J. Whitehouse, A.M. Martino, P.G. Antuono, P.R. Lowenstein, J.T. Coyle, D.L. Price, K.J. Kellar: Nicotinic acetylcholine binding sites in Alzheimer's disease. *Brain Res* 371, 146-51 (1986)

48. A. Nordberg, H. Lundqvist, P. Hartvig, A. Lilja, B. Langstrom: Kinetic analysis of regional (S)-11C-nicotine binding in normal and Alzheimer brains--in vivo assessment using positron emission tomography. *Alzheimer Dis Assoc Disord* 9, 21-7 (1995)

49. C. Halldin, K. Nagren, C.G. Swahn, B. Langstrom, H. Nyback: (S)- and (R)-[11C]nicotine and the metabolite (R/S)-[11C]cotinine. Preparation, metabolite studies and in vivo distribution in the human brain using PET. *Int J Rad Appl Instrum B* 19, 871-80 (1992)

50. H. Nyback, C. Halldin, A. Ahlin, M. Curvall, L. Eriksson: PET studies of the uptake of (S)- and (R)-[11C]nicotine in the human brain: difficulties in visualizing specific receptor binding in vivo. *Psychopharmacology (Berl)* 115, 31-6 (1994)

51. J.A. Court, M.A. Piggott, S. Lloyd, N. Cookson, C.G. Ballard, I.G. McKeith, R.H. Perry, E.K. Perry: Nicotine binding in human striatum: elevation in schizophrenia and reductions in dementia with Lewy bodies, Parkinson's disease and Alzheimer's disease and in relation to neuroleptic medication. *Neuroscience* 98, 79-87 (2000)

52. A. Horti, H.T. Ravert, E.D. London, R.F. Dannals: Synthesis of a radiotracer for studying nicotinic acetylcholine receptors: (+/-)-exo-2-(2-[18F]fluoro-5-pyridyl)-7-azabicyclo[2.2.1]heptane. *J Labelled Comp Radiopharm* 38, 355-65 (1996)

53. M. Maziere, J. Delforge: PET imaging [11C]nicotine: historical aspects. In: Domino E (ed) Brain imaging of nicotine and tobacco smoking. *NPP Books, Ann Arbor*, 13-28 (1995)

54. B. Badio, J.W. Daly: Epibatidine, a potent analgetic and nicotinic agonist. *Mol Pharmacol* 45, 563-9 (1994)

55. C. Qian, T. Li, T.Y. Shen, L. Libertine-Garahan, J. Eckman, T. Biftu, S. Ip: Epibatidine is a nicotinic analgesic. *Eur J Pharmacol* 250, R13-4 (1993)

56. M. Dukat, R.A. Glennon: Epibatidine: impact on nicotinic receptor research. *Cell Mol Neurobiol* 23, 365-78 (2003)

57. D.W. Bonhaus, K.R. Bley, C.A. Broka, D.J. Fontana, E. Leung, R. Lewis, A. Shieh, E.H. Wong: Characterization of the electrophysiological, biochemical and behavioral actions of epibatidine. *J Pharmacol Exp Ther* 272, 1199-203 (1995)

58. A. Horti, U. Scheffel, M. Stathis, P. Finley, H.T. Ravert, E.D. London, R.F. Dannals: Fluorine-18-FPH for PET imaging of nicotinic acetylcholine receptors. *J Nucl Med* 38, 1260-5 (1997)

59. E.D. London, U. Scheffel, A.S. Kimes, K.J. Kellar: In vivo labeling of nicotinic acetylcholine receptors in brain with [3H]epibatidine. *Eur J Pharmacol* 278, R1-2 (1995)

60. P.E. Molina, Y.S. Ding, F.I. Carroll, F. Liang, N.D. Volkow, N. Pappas, M. Kuhar, N. Abumrad, S.J. Gatley, J.S. Fowler: Fluoro-norchloroepibatidine: preclinical assessment of acute toxicity. *Nucl Med Biol* 24, 743-7 (1997)

61. A.O. Koren, A.G. Horti, A.G. Mukhin, D. Gundisch, A.S. Kimes, R.F. Dannals, E.D. London: 2-, 5-, and 6-Halo-3-(2(S)-azetidinylmethoxy)pyridines: synthesis, affinity for nicotinic acetylcholine receptors, and molecular modeling. *J Med Chem* 41, 3690-8 (1998)

62. J.P. Sullivan, D. Donnelly-Roberts, C.A. Briggs, D.J. Anderson, M. Gopalakrishnan, M. Piattoni-Kaplan, J.E. Campbell, D.G. McKenna, E. Molinari, A.M. Hettinger, D.S. Garvey, J.T. Wasicak, M.W. Holladay, M. Williams, S.P. Arneric: A-85380 [3-(2(S)-azetidinylmethoxy) pyridine]: in vitro pharmacological properties of a novel, high affinity α4β2 nicotinic acetylcholine receptor ligand. *Neuropharmacology* 35, 725-34 (1996)

63. U. Scheffel, A.G. Horti, A.O. Koren, H.T. Ravert, J.P. Banta, P.A. Finley, E.D. London, R.F. Dannals: 6-[18F]Fluoro-A-85380: an in vivo tracer for the nicotinic acetylcholine receptor. *Nucl Med Biol* 27, 51-6 (2000)

64. A.G. Horti, U. Scheffel, A.O. Koren, H.T. Ravert, W.B. Mathews, J.L. Musachio, P.A. Finley, E.D. London, R.F. Dannals: 2-[18F]Fluoro-A-85380, an in vivo tracer for the nicotinic acetylcholine receptors. *Nucl Med Biol* 25, 599-603 (1998)

65. W. Sihver, A. Nordberg, B. Langstrom, A.G. Mukhin, A.O. Koren, A.S. Kimes, E.D. London: Development of ligands for in vivo imaging of cerebral nicotinic receptors. *Behav Brain Res* 113, 143-57 (2000)

66. Y. Ding, N. Liu, T. Wang, J. Marecek, V. Garza, I. Ojima, J.S. Fowler: Synthesis and evaluation of 6-

[^{18}F]fluoro-3-(2(S)-azetidinylmethoxy)pyridine as a PET tracer for nicotinic acetylcholine receptors. *Nucl Med Biol* 27, 381-9 (2000)

67. A.G. Horti, S.I. Chefer, A.G. Mukhin, A.O. Koren, D. Gundisch, J.M. Links, V. Kurian, R.F. Dannals, E.D. London: 6-[^{18}F]fluoro-A-85380, a novel radioligand for in vivo imaging of central nicotinic acetylcholine receptors. *Life Sci* 67, 463-9 (2000)

68. Y.S. Ding, J.S. Fowler, J. Logan, G.J. Wang, F. Telang, V. Garza, A. Biegon, D. Pareto, W. Rooney, C. Shea, D. Alexoff, N.D. Volkow, F. Vocci: 6-[^{18}F]Fluoro-A-85380, a new PET tracer for the nicotinic acetylcholine receptor: studies in the human brain and in vivo demonstration of specific binding in white matter. *Synapse* 53, 184-9 (2004)

69. J.K. Staley, C.H. van Dyck, D. Weinzimmer, E. Brenner, R.M. Baldwin, G.D. Tamagnan, P. Riccardi, E. Mitsis, J.P. Seibyl: ^{123}I-5-IA-85380 SPECT Measurement of Nicotinic Acetylcholine Receptors in Human Brain by the Constant Infusion Paradigm: Feasibility and Reproducibility. *J Nucl Med* 46, 1466-72 (2005)

70. Y. Ding, N. Liu, J. Logan, V. Garza, C. Shea, R. Macgregor, J. Fowler, N. Volkow: Comparative PET studies of nicotinic acetylcholine receptors using 2- and 6-[^{18}F]fluoro-3-(2-(S)-azetidinylmethoxy)-pyridine. *J Nucl Med* 41(Suppl), 212P (2000)

71. M. Bottlaender, H. Valette, D. Roumenov, F. Dolle, C. Coulon, M. Ottaviani, F. Hinnen, M. Ricard: Biodistribution and radiation dosimetry of ^{18}F-fluoro-A-85380 in healthy volunteers. *J Nucl Med* 44, 596-601 (2003)

72. D. Gundisch, A.O. Koren, A.G. Horti, O.A. Pavlova, A.S. Kimes, A.G. Mukhin, E.D. London: In vitro characterization of 6-[^{18}F]fluoro-A-85380, a high-affinity ligand for α4β2 nicotinic acetylcholine receptors. *Synapse* 55, 89-97 (2005)

73. G.G. Glenner, C.W. Wong: Alzheimer's disease: initial report of the purification and characterization of a novel cerebrovascular amyloid protein. *Biochem Biophys Res Commun* 120, 885-90 (1984)

74. P.D. Gorevic, F. Goni, B. Pons-Estel, F. Alvarez, N.S. Peress, B. Frangione: Isolation and partial characterization of neurofibrillary tangles and amyloid plaque core in Alzheimer's disease: immunohistological studies. *J Neuropathol Exp Neurol* 45, 647-64 (1986)

75. C.L. Masters, G. Simms, N.A. Weinman, G. Multhaup, B.L. McDonald, K. Beyreuther: Amyloid plaque core protein in Alzheimer disease and Down syndrome. *Proc Natl Acad Sci U S A* 82, 4245-9 (1985)

76. S. Estus, T.E. Golde, T. Kunishita, D. Blades, D. Lowery, M. Eisen, M. Usiak, X.M. Qu, T. Tabira, B.D. Greenberg, et al.: Potentially amyloidogenic, carboxyl-terminal derivatives of the amyloid protein precursor. *Science* 255, 726-8 (1992)

77. S.S. Sisodia: Beta-amyloid precursor protein cleavage by a membrane-bound protease. *Proc Natl Acad Sci U S A* 89, 6075-9 (1992)

78. T.E. Golde, S. Estus, L.H. Younkin, D.J. Selkoe, S.G. Younkin: Processing of the amyloid protein precursor to potentially amyloidogenic derivatives. *Science* 255, 728-30 (1992)

79. J. Kang, H.G. Lemaire, A. Unterbeck, J.M. Salbaum, C.L. Masters, K.H. Grzeschik, G. Multhaup, K. Beyreuther, B. Muller-Hill: The precursor of Alzheimer's disease amyloid A4 protein resembles a cell-surface receptor. *Nature* 325, 733-6 (1987)

80. E. Storey, R. Cappai: The amyloid precursor protein of Alzheimer's disease and the Abeta peptide. *Neuropathol Appl Neurobiol* 25, 81-97 (1999)

81. M. Goedert: Neurofibrillary pathology of Alzheimer's disease and other tauopathies. *Prog Brain Res* 117, 287-306 (1998)

82. J.E. Maggio, P.W. Mantyh: Brain amyloid--a physicochemical perspective. *Brain Pathol* 6, 147-62 (1996)

83. A.M. Manelli, P.S. Puttfarcken: β-Amyloid-induced toxicity in rat hippocampal cells: in vitro evidence for the involvement of free radicals. *Brain Res Bull* 38, 569-76 (1995)

84. D.T. Weldon, S.D. Rogers, J.R. Ghilardi, M.P. Finke, J.P. Cleary, E. O'Hare, W.P. Esler, J.E. Maggio, P.W. Mantyh: Fibrillar beta-amyloid induces microglial phagocytosis, expression of inducible nitric oxide synthase, and loss of a select population of neurons in the rat CNS in vivo. *J Neurosci* 18, 2161-73 (1998)

85. J.C. Vickers, T.C. Dickson, P.A. Adlard, H.L. Saunders, C.E. King, G. McCormack: The cause of neuronal degeneration in Alzheimer's disease. *Prog Neurobiol* 60, 139-65 (2000)

86. N.P. Verhoeff, A.A. Wilson, S. Takeshita, L. Trop, D. Hussey, K. Singh, H.F. Kung, M.P. Kung, S. Houle: In-vivo imaging of Alzheimer disease β-amyloid with [^{11}C]SB-13 PET. *Am J Geriatr Psychiatry* 12, 584-95 (2004)

87. K. Shoghi-Jadid, G.W. Small, E.D. Agdeppa, V. Kepe, L.M. Ercoli, P. Siddarth, S. Read, N. Satyamurthy, A. Petric, S.C. Huang, J.R. Barrio: Localization of neurofibrillary tangles and beta-amyloid plaques in the brains of living patients with Alzheimer disease. *Am J Geriatr Psychiatry* 10, 24-35 (2002)

88. W.E. Klunk, H. Engler, A. Nordberg, Y. Wang, G. Blomqvist, D.P. Holt, M. Bergstrom, I. Savitcheva, G.F. Huang, S. Estrada, B. Ausen, M.L. Debnath, J. Barletta, J.C. Price, J. Sandell, B.J. Lopresti, A. Wall, P. Koivisto, G. Antoni, C.A. Mathis, B. Langstrom: Imaging brain amyloid in Alzheimer's disease with Pittsburgh Compound-B. *Ann Neurol* 55, 306-19 (2004)

89. T.T. Ashburn, H. Han, B.F. McGuinness, P.T. Lansbury, Jr.: Amyloid probes based on Congo Red distinguish between fibrils comprising different peptides. *Chem Biol* 3, 351-8 (1996)

90. W.E. Klunk, J.W. Pettegrew, D.J. Abraham: Quantitative evaluation of congo red binding to amyloid-like proteins with a β-pleated sheet conformation. *J Histochem Cytochem* 37, 1273-81 (1989)

91. W.E. Klunk, M.L. Debnath, J.W. Pettegrew: Development of small molecule probes for the β-amyloid protein of Alzheimer's disease. *Neurobiol Aging* 15, 691-8 (1994)

92. C.A. Mathis, K. Mahmood, M.L. Debnath, W.E. Klunk: Synthesis of a lipophilic, radioiodinated ligand with high affinity to amyloid protein in Alzheimer's disease brain tissue. *J Labelled Compd Radiopharm* 39, 594-5 (1997)

93. N.A. Dezutter, R.J. Dom, T.J. de Groot, G.M. Bormans, A.M. Verbruggen: ^{99m}Tc-MAMA-chrysamine G, a probe

for beta-amyloid protein of Alzheimer's disease. *Eur J Nucl Med* 26, 1392-9 (1999)

94. W. Zhen, H. Han, M. Anguiano, C.A. Lemere, C.G. Cho, P.T. Lansbury, Jr.: Synthesis and amyloid binding properties of rhenium complexes: preliminary progress toward a reagent for SPECT imaging of Alzheimer's disease brain. *J Med Chem* 42, 2805-15 (1999)

95. Z.P. Zhuang, M.P. Kung, C. Hou, D.M. Skovronsky, T.L. Gur, K. Plossl, J.Q. Trojanowski, V.M. Lee, H.F. Kung: Radioiodinated styrylbenzenes and thioflavins as probes for amyloid aggregates. *J Med Chem* 44, 1905-14 (2001)

96. M.P. Kung, C. Hou, Z.P. Zhuang, D. Skovronsky, H.F. Kung: Binding of two potential imaging agents targeting amyloid plaques in postmortem brain tissues of patients with Alzheimer's disease. *Brain Res* 1025, 98-105 (2004)

97. W. Zhang, S. Oya, M.P. Kung, C. Hou, D.L. Maier, H.F. Kung: F-18 stilbenes as PET imaging agents for detecting β-amyloid plaques in the brain. *J Med Chem* 48, 5980-8 (2005)

98. M. Ono, A. Wilson, J. Nobrega, D. Westaway, P. Verhoeff, Z.P. Zhuang, M.P. Kung, H.F. Kung: ^{11}C-labeled stilbene derivatives as Aβ-aggregate-specific PET imaging agents for Alzheimer's disease. *Nucl Med Biol* 30, 565-71 (2003)

99. C.A. Mathis, B.J. Bacskai, S.T. Kajdasz, M.E. McLellan, M.P. Frosch, B.T. Hyman, D.P. Holt, Y. Wang, G.F. Huang, M.L. Debnath, W.E. Klunk: A lipophilic thioflavin-T derivative for positron emission tomography (PET) imaging of amyloid in brain. *Bioorg Med Chem Lett* 12, 295-8 (2002)

100. C.A. Mathis, Y. Wang, D.P. Holt, G.F. Huang, M.L. Debnath, W.E. Klunk: Synthesis and evaluation of ^{11}C-labeled 6-substituted 2-arylbenzothiazoles as amyloid imaging agents. *J Med Chem* 46, 2740-54 (2003)

101. W.E. Klunk, Y. Wang, G.F. Huang, M.L. Debnath, D.P. Holt, C.A. Mathis: Uncharged thioflavin-T derivatives bind to amyloid-β protein with high affinity and readily enter the brain. *Life Sci* 69, 1471-84 (2001)

102. Y. Wang, W.E. Klunk, G.F. Huang, M.L. Debnath, D.P. Holt, C.A. Mathis: Synthesis and evaluation of 2-(3'-iodo-4'-aminophenyl)-6-hydroxybenzothiazole for in vivo quantitation of amyloid deposits in Alzheimer's disease. *J Mol Neurosci* 19, 11-6 (2002)

103. R.J. Bateman, D. Eidelberg: Testing a test for Alzheimer disease. *Neurology* 68, 482-3 (2007)

104. D.R. Thal, U. Rub, M. Orantes, H. Braak: Phases of A beta-deposition in the human brain and its relevance for the development of AD. *Neurology* 58, 1791-800 (2002)

105. S.E. Arnold, B.T. Hyman, J. Flory, A.R. Damasio, G.W. Van Hoesen: The topographical and neuroanatomical distribution of neurofibrillary tangles and neuritic plaques in the cerebral cortex of patients with Alzheimer's disease. *Cereb Cortex* 1, 103-16 (1991)

106. Z.P. Zhuang, M.P. Kung, C. Hou, K. Plossl, D. Skovronsky, T.L. Gur, J.Q. Trojanowski, V.M. Lee, H.F. Kung: IBOX(2-(4'-dimethylaminophenyl)-6-iodobenzoxazole): a ligand for imaging amyloid plaques in the brain. *Nucl Med Biol* 28, 887-94 (2001)

107. Z.P. Zhuang, M.P. Kung, A. Wilson, C.W. Lee, K. Plossl, C. Hou, D.M. Holtzman, H.F. Kung: Structure-activity relationship of imidazo[1,2-a]pyridines as ligands for detecting beta-amyloid plaques in the brain. *J Med Chem* 46, 237-43 (2003)

108. M.P. Kung, C. Hou, Z.P. Zhuang, A.J. Cross, D.L. Maier, H.F. Kung: Characterization of IMPY as a potential imaging agent for beta-amyloid plaques in double transgenic PSAPP mice. *Eur J Nucl Med Mol Imaging* 31, 1136-45 (2004)

109. E.D. Agdeppa, V. Kepe, J. Liu, S. Flores-Torres, N. Satyamurthy, A. Petric, G.M. Cole, G.W. Small, S.C. Huang, J.R. Barrio: Binding characteristics of radiofluorinated 6-dialkylamino-2-naphthylethylidene derivatives as positron emission tomography imaging probes for beta-amyloid plaques in Alzheimer's disease. *J Neurosci* 21, RC189 (2001)

110. J.R. Barrio, S.C. Huang, G. Cole, N. Satyamurthy, A. Petric, M.E. Phelps, G. Small: PET imaging of tangles and plaques in Alzheimer disease with a highly hydrophobic probe. *J Labelled Compd Radiopharm* 42, S194-5 (1999)

111. C. Bancher, H. Braak, P. Fischer, K.A. Jellinger: Neuropathological staging of Alzheimer lesions and intellectual status in Alzheimer's and Parkinson's disease patients. *Neurosci Lett* 162, 179-82 (1993)

112. G.W. Small, V. Kepe, L.M. Ercoli, P. Siddarth, S.Y. Bookheimer, K.J. Miller, H. Lavretsky, A.C. Burggren, G.M. Cole, H.V. Vinters, P.M. Thompson, S.C. Huang, N. Satyamurthy, M.E. Phelps, J.R. Barrio: PET of brain amyloid and tau in mild cognitive impairment. *N Engl J Med* 355, 2652-63 (2006)

113. A. Drzezga, M. Riemenschneider, B. Strassner, T. Grimmer, M. Peller, A. Knoll, S. Wagenpfeil, S. Minoshima, M. Schwaiger, A. Kurz: Cerebral glucose metabolism in patients with AD and different APOE genotypes. *Neurology* 64, 102-7 (2005)

114. E.M. Reiman, R.J. Caselli, L.S. Yun, K. Chen, D. Bandy, S. Minoshima, S.N. Thibodeau, D. Osborne: Preclinical evidence of Alzheimer's disease in persons homozygous for the epsilon 4 allele for apolipoprotein E. *N Engl J Med* 334, 752-8 (1996)

115. G.W. Small, L.M. Ercoli, D.H. Silverman, S.C. Huang, S. Komo, S.Y. Bookheimer, H. Lavretsky, K. Miller, P. Siddarth, N.L. Rasgon, J.C. Mazziotta, S. Saxena, H.M. Wu, M.S. Mega, J.L. Cummings, A.M. Saunders, M.A. Pericak-Vance, A.D. Roses, J.R. Barrio, M.E. Phelps: Cerebral metabolic and cognitive decline in persons at genetic risk for Alzheimer's disease. *Proc Natl Acad Sci U S A* 97, 6037-42 (2000)

116. E.F. de Vries: Imaging of cyclooxygenase-2 (COX-2) expression: potential use in diagnosis and drug evaluation. *Curr Pharm Des* 12, 3847-56 (2006)

117. X. Liang, Q. Wang, T. Hand, L. Wu, R.M. Breyer, T.J. Montine, K. Andreasson: Deletion of the prostaglandin E2 EP2 receptor reduces oxidative damage and amyloid burden in a model of Alzheimer's disease. *J Neurosci* 25, 10180-7 (2005)

Abbreviations: Alzheimer's disease (AD), central nervous system (CNS), acetylcholinesterase (AChE), choline acetyltransferase (ChAT), acetylcholine (ACh), nicotinic acetylcholine receptor (nAChR), positron emission tomography (PET), single-photon emission computed tomography (SPECT), blood-brain barrier (BBB), N-[^{11}C]methylpiperidin-4-yl acetate ([^{11}C]AMP), N-

[^{11}C]methylpiperidin-4-yl propionate ([^{11}C]PMP), butyrylcholinesterase (BuChE), 5,7-dihydro-3-[2-[1-(phenylmethyl]-4-piperidinyl]ethyl]-6*H*-pyrrolo[3,2-*f*]-1,2-benzisoxazol-6-one (CP-118,954) and 5,7-dihydro-7-methyl-3-[2-[1-(phenylmethyl]-4-piperidinyl]ethyl]-6*H*-pyrrolo[3,2-*f*]-1,2-benzisoxazol-6-one (CP-126,998), (+/-)-exo-2-(2-[^{18}F]fluoro-5-pyridyl)-7-azabicyclo[2.2.1]heptane ([^{18}F]FPH), 3-[2(S)-2-azetidinylmethoxy]pyridine (A-85380), Chrysamine G (CG), Congo red (CR), (E,E)-1-iodo-2,5-bis(3-hydroxycarbonyl-4-hydroxy)styrylbenzene (ISB), and (E,E)-1-iodo-2,5-bis(3-hydroxycarbonyl-4-methoxy)styrylbenzene, (IMSB), 4-N-methylamino-4'-hydroxystilbene (SB-13), benzothiazole aniline (BTA), [N-methyl-^{11}C]-2-(4'-methylaminophenyl)-6-hydroxylbenzothiazole ([^{11}C]6-OH-BTA-1, Pittsburgh Compound-B' or simply, PIB), 2-[4'-(dimethylamino)phenyl]-6-iodobenzothiazole (TZDM), 2-[4'-(4"-methylpiperazin-1-yl)phenyl]-6-iodobenzothiazole (TZPI), 2-(4'-dimethylaminophenyl)-6-iodobenzoxazole (IBOX), 6-iodo-2-(4'-dimethylamino-)phenyl-imidazo[1,2-a]pyridine (IMPY), 2-(1-(6-[(2-fluoroethyl)(methyl)amino]-2-naphthyl)ethylidene)malononitrile (FDDNP), 1-(6-[(2-fluoroethyl)(methyl)amino]-naphthalene-2-yl)ethanone (FENE), apolipoprotein E (ApoE)

Key Words: Alzheimer's disease, Acetylcholinesterase, Nicotinic Acetylcholine Receptor, β-Amyloid Plaques, Neurofibrillary Tangles, PET, SPECT, Review

Send correspondence to: Xiaoyuan Chen, PhD, the Molecular Imaging Program at Stanford (MIPS), Department of Radiology and Bio-X Program, Stanford University School of Medicine, 1201 Welch Rd, P095, Stanford, CA 94305, Tel: 650-725-0950, Fax: 650-736-7925, E-mail: shawchen@stanford.edu